4570 *Inorg. Chem.* **2010**, *49*, 4570–4577
DOI: 10.1021/ic100118q

Inorganic Chemistry
Article

$M_3(Au,Ge)_{19}$ and $M_{3.25}(Au,Ge)_{18}$ (M = Ca, Yb): Distinctive Phase Separations Driven by Configurational Disorder in Cubic YCd_6-Type Derivatives

Qisheng Lin and John D. Corbett*

Department of Chemistry, Iowa State University, Ames, Iowa 50010

Received January 19, 2010

Exploratory syntheses in the M−Au−Ge (M = Ca, Yb) systems have led to the discovery of two cleanly separated nonstoichiometric phases $M_3Au_{\sim 14.4}Ge_{\sim 4.6}$ (**I**) and $M_{3.25}Au_{\sim 12.7}Ge_{\sim 5.3}$ (**II**). Single crystal X-ray studies reveal that both (space group $Im\bar{3}$) feature body-centered-cubic packing of five-shell multiply endohedral clusters that resemble those in the parent YCd_6 (= Y_3Cd_{18}) and are akin to approximate phases in other quasicrystal systems. However, differences resulting from various disorders in these are distinctive. The innermost cluster in the $M_3Au_{\sim 14.4}Ge_{\sim 4.6}$ phase (**I**) remains a disordered tetrahedron, as in the YCd_6 parent. In contrast, its counterpart in the electron-richer $M_{3.25}Au_{\sim 12.7}Ge_{\sim 5.3}$ phase (**II**) is a "rattling" M atom. The structural differentiations between **I** and **II** exhibit strong correlations between lattice parameters, cluster sizes, particular site occupancies, and valence electron counts.

Introduction

Quasiperiodic crystals (QCs),[1] or quasicrystals in short, exhibit potential applications in advanced technological materials, for example, surface coatings,[2] catalysts,[3] thermoelectrics,[4] hydrogen storage,[5] photonic crystals,[6] and bioinspired materials.[7] Recently, exploratory syntheses of these unusual materials have aroused the interest of a few chemists.[8−12] However, knowledge of QC structures still lag much behind because classic crystallography cannot handle crystal structures with quasiperiodicity,[1] which exhibit self-similarity upon inflation/deflation on τ (the golden mean, 1.618) and lack translational periodicity. In particular, an icosahedral QC (i-QC) has quasiperiodicity in three-dimensions, requiring six-dimensional crystallography to fully characterize its structure. Thus, the so-called crystalline approximant (AC) neighbors play important roles in modeling QC structures and in rationalizing the structure−property relationships of QCs. ACs are conventional crystals, and they are assumed to contain local atomic clusters similar to those found in corresponding QC. In addition, the structure and bonding analyses of various ACs provide an ideal playground for chemists to probe relationships among polar intermetallics, Hume−Rothery, and Zintl phases.

In the past 10 years, YCd_6-type[13] compounds have received renewed interest[10,11,14−19] because the isostructural $CaCd_6$ and $YbCd_6$ were found to be 1/1 ACs[20] of their QCs, $CaCd_{5.67}$ and $YbCd_{5.67}$,[21,22] respectively. The building blocks of YCd_6-type structures are five-shell multiply endohedral clusters, each one of which is ordered from the center out as a disordered tetrahedron (4 atoms total), a pentagonal dodecahedron (20), an icosahedron (12), an icosidodecahedron (30), and an outermost triacontahedron (32 + 60). However, recent studies have revealed that various disorders may exist in YCd_6-type structures.[10,11,14,16−19] Particularly, they may contain orientation disorder of the innermost tetrahedron, deformation or disorder of the dodecahedron (including split positions), and occupation of an additional special Wyckoff 8*c* site (1/4, 1/4, 1/4). (Strictly speaking, occupation at the last position results in a

*To whom correspondence should be addressed. E-mail: jcorbett@iastate.edu.

(1) Janot, C. *Quasicrystals: A Primer*, 2nd ed.; Oxford University Press: Oxford, U.K., 1994.
(2) Rivier, N. *J. Non-Cryst. Solids* **1993**, *153−154*, 458.
(3) Kameoka, S.; Tanabe, T.; Tsai, A. P. *Catal. Today* **2004**, *93−95*, 23.
(4) Macia, E. *Appl. Phys. Lett.* **2000**, *77*, 3045.
(5) Kelton, K. F.; Gibbons, P. C. *MRS Bull.* **1997**, *22*, 71.
(6) Freedman, B.; Bartal, G.; Segev, M; Lifshitz, R.; Christodoulides, D. N.; Fleischer, J. W. *Nature* **2006**, *446*, 1166.
(7) Andersen, B. C.; Bloom, P. D.; Baikerikar, K. G.; Sheares, V. V.; Mallapragada, S. K. *Biomaterials* **2002**, *23*, 1761.
(8) Conrad, M.; Harbrecht, B. *Chem.—Eur. J.* **2002**, *8*, 3093.
(9) Tsai, A. P. *Acc. Chem. Res.* **2003**, *36*, 31.
(10) Pay Gómez, C.; Lidin, S. *Phys. Rev. B* **2003**, *68*, 024203.
(11) Piao, S.; Gomez, C. P.; Lidin, S. *Z. Naturforsch.* **2006**, *61b*, 644.
(12) Lin, Q.; Corbett, J. D. *Struct. Bonding* (*Berlin*) **2009**, *133*, 1.
(13) Larson, A. C.; Cromer, D. T. *Acta Crystallogr.* **1971**, *27B*, 1875.
(14) Lin, Q.; Corbett, J. D. *Inorg. Chem.* **2004**, *43*, 1912.
(15) Ishimasa, T.; Kaneko, Y.; Kaneko, H. *J. Non-Cryst. Solids* **2004**, *334&335*, 1.
(16) Lin, Q.; Corbett, J. D. *J. Am. Chem. Soc.* **2005**, *127*, 12786.
(17) Lin, Q.; Corbett, J. D. *J. Am. Chem. Soc.* **2006**, *128*, 13268.
(18) Lin, Q.; Corbett, J. D. *J. Am. Chem. Soc.* **2007**, *129*, 6789.
(19) Lin, Q.; Corbett, J. D. *Inorg. Chem.* **2008**, *47*, 7651.
(20) 1/1 AC denotes an order of the cubic AC. According to high dimensional crystallography, the cell parameters of a q/p cubic AC ($a_{q/p}$) is related to the QC lattice constant (a_6, indexed in six dimensions) by $a_{q/p} = 2a_6(p + q\tau)/(2 + \tau)^{1/2}$, in which τ is the golden mean, and p and q are two consecutive Fibonacci numbers (1, 1, 2, 3, 5, 8, 13, 21, ...)[1].
(21) Tsai, A. P.; Guo, J. Q.; Abe, E.; Takakura, H.; Sato, T. J. *Nature* **2000**, *408*, 537.
(22) Takakura, H.; Pay Gómez, C.; Yamamoto, Y.; De Boissieu, M.; Tsai, A. P. *Nat. Mater.* **2007**, *6*, 58.

 Published on Web 04/14/2010

Table 1. Some Reaction Compositions, Products, and Refined Lattice Constants for YCd_6-Type Phases in the M−Au−Ge (M = Ca and Yb) Systems

				lattice constants[c]		
code	proportion (%)	conditions[a]	products and estimated yields[b]	powder data	single crystal data	crystals
	Ca/Au/Ge					
1	14.3/64.3/21.4	940/500	75% YC_t + 20% YC_s+ U_1	14.7620(5), 14.6805(5)	14.766(1)	
2	14.4/62.5/23.1	900/500	70% YC_t + 30% YC_s	14.7669(5),14.6801(5)		
3	14.3/60.7/25.0	850/400	70% YC_s + 30% YC_t	14.7676(5), 14.8305(5)	**14.764(5), 14.8315(9)**	**3, 5**
4	14.2/59.1/26.7	850/500	>98% YC_s	14.7053(5)	**14.712(1)**	**2**
5	14.3/57.1/28.6	850/500	>98% % YC_s	14.6838(5)	**14.6843(9)**	**s1**
6	14.3/50.0/35.7	940/500	55% YC_s+ 15% $CaAu_2Ge_2$ +30% Ge	14.6760(5)	**14.670(1)**	**1**
7	10.0/65.0/25.0	850/400	>98% YC_t	14.8200(5)	**14.822(1)**	**s2**
8	10.0/60.0/30.0	850/400	60% YC_t + 35% Ge + U_2	14.8063(5)	**14.805(1)**	**4**
9	10.0/50.0/40.0	850/400	50% YC_t+ 40% Ge + U_2	14.8051(5)	14.807(2)	
10	20.0/55.0/25.0	850/400	20% YC_s + 10% $CaAu_3Ge$+ 60% $Ca_3(Au,Ge)_{11}$+ 10% CaAuGe	14.6904(5)		
11	20.0/50.0/30.0	850/400	15% YC_s+ 70% $Ca_3(Au,Ge)_{11}$ + 15% CaAuGe	14.6810(5)	14.682(1)	
	Yb/Au/Ge					
12	14.3/50.0/35.7	900/500	55% YC_s + 45% U_3	14.6288(5)	**14.6334(9)**	**s3**
13	10.0/65.0/35.0	900/500	70% YC_t + 30% YC_s	14.7678(5), 14.6278(5)	**14.769(2)**	**s4**
14	14.5/62.0/23.5	900/500	55% YC_t + 45% YC_s	14.7675(5), 14.6692(5)		
15	15.3/58.9/25.9	900/500	40% YC_t + 60% YC_s	14.7663(5), 14.6235(5)		

[a] The heating and annealing temperatures (°C) are listed. The ramp speed and duration time are same for all reactions, as in the text. [b] The percentages were estimated according to observed peak intensities in powder patterns. YC_s and YC_t denote YCd_6-type derivatives that are centered by a single atom (**II**) and a tetrahedron (**I**), respectively. U_i (i = 1, 2, 3) denote different unknown phases. [c] Lattice parameters from powder data were refined from five to nine of the strongest peaks within 20°−70°, if discernible, whereas single crystal data were refined from all observed reflections [$I > 2\sigma(I)$]. Bold numbers representing lattice parameters for single crystal structures are reported in the text and coded in the last column.

change of structural type, but for convenience these may still be considered as YCd_6-type derivatives.)

These disorders are not separate phenomena; rather, they exhibit strong correlations. A comprehensive study on MCd_6 (M = rare-earth metal) by Lidin and co-workers[11] revealed that the orientation of the tetrahedron strongly depends on the size of the M metal. A large M expands the polyhedral shells and results in a remarkable diversity of disorders around the tetrahedron as well as occupation of the additional 8*c* sites. Further, they showed that the presence of atoms at 8*c* sites correlates with the deformation of the neighboring dodecahedron and the orientation of the innermost tetrahedron as well. Recently, Fornasini and co-workers[23] reported another apparent disorder type, that the building blocks in $YbZn_{5.86}$ and $Yb(Zn,Al)_{5.75}$ include both a fractional single Yb atom and a disordered tetrahedron within the dodecahedral shell, a rare case.

During continued development of QC systems, we have discovered 1/0, 1/1, and 2/1 ACs and i-QC phases in the Ca−Au−Ga system.[19,24] The valence electron count per atom in the $Ca_{15.2(5)}Au_{50.2(6)}Ga_{34.5(4)}$ i-QC (e/a = 1.84) is notably lower than usual (~2.0), suggesting that substitution of Ga by electron-richer elements (e.g., Ge or Sn) might be a promising electronic way to tune i-QCs and ACs. Moreover, explorations of Ca−Au−Ge/Sn systems might illustrate whether low lying d orbitals on the electropositive element differentiate the formation of YCd_6[13] and $Mg_{32}(Al,Zn)_{49}$[25] type AC structures, noting that both $Na_{52}Au_{80}Ge_{30}$ and $Na_{60}Au_{78}Sn_{24}$[26] are isostructural with the latter AC structure. Recently, we also reported the syntheses and structures of two La_3Al_{11} type $Ca_3Au_{11-x}Ge_x$ phases (*Imm*2: ~ 7.0 < x < 7.5; *Pnnm*: 7.5 < x < ~8.0)[27] that are neighbors of the present $Ca_3(Au,Ge)_{19}$ and $Ca_{3.25}(Au,Ge)_{18}$. In this work, we report the syntheses and structures of two distinctively different YCd_6-type derivatives in the M−Au−Ge (M = Ca, Yb) systems: One contains a disordered tetrahedron and the other, only a fractional single M atom, as the innermost units in the multiply endohedral clusters. The appearance of both derivatives in a same system is the main novelty. The two phases show pronounced distinctions regarding lattice parameters, compositions, disorders, and valence electron counts. Parallel explorations of the M−Au−Sn (M = Ca, Yb) systems yield very different results, which will be reported separately.[28]

Experimental Section

Synthesis. High purity elements as Ca chunks, Yb particles, Au sheets, and Ge particles (all >99.99%, Alfa-Aesar) were weighed in a N_2-filled glovebox (H_2O < 0.1 ppm vol.) and weld-sealed under Ar into Ta containers. The last were in turn enclosed in evacuated SiO_2 jackets (< 10^{-6} Torr) to avoid air oxidation at elevated temperature.

Reactions $CaAu_{6-x}Ge_x$ (x = 3.5, 4.0, 4.5, 5.0) were first designed to check the availability of a YCd_6-type phase in the Ca−Au−Ge system. Exploratory samples were heated at 940 °C for 24 h, cooled to 500 °C at a rate of 2 °C/h, annealed there for three weeks, and then quenched into water. To examine phase widths of the target phases, reactions with the previously refined stoichiometries and wider composition ranges (Table 1) were reacted under similar conditions: heated at 850 or 900 °C for 24 h, and then slowly cooled to and annealed at 400 or 500 °C for 3 w. Also, a routine check of the availability of a Ca−Au−Ge i-QC phase was made by repeating reactions 4 and 5, but quenching the samples directly from 850 °C. However, no i-QC phase was detected on the basis of powder pattern

(23) Fornasini, M. L.; Manfrinetti, P.; Mazzone, D.; Dhar, S. K. *Z. Naturforsch.* **2008**, *63b*, 237.
(24) Lin, Q.; Corbett, J. D. *Inorg. Chem.* **2008**, *47*, 3462.
(25) Bergman, G.; Waugh, J. L. T.; Pauling, L. *Acta Crystallogr.* **1957**, *10*, 254.
(26) Doering, W.; Seelentag, W.; Buchholz, W.; Schuster, H. U. *Z. Naturforsch.* **1979**, *34b*, 1715.
(27) Lin, Q.; Corbett, J. D. *Inorg. Chem.* **2009**, *48*, 5403.
(28) Lin, Q.; Corbett, J. D., unpublished results.

Table 2. Some Data Collection and Refinement Parameters for YCd_6-Type Ca−Au−Ge (**1**−**5**) Structures

crystal	**1**	**2**	**3**	**4**	**5**
formula	$Ca_{3.25}Au_{12.50}Ge_{5.50}$	$Ca_{3.25}Au_{12.94(3)}Ge_{5.06(2)}$	$Ca_{3.05(2)}Au_{13.69(8)}Ge_{5.31(6)}$	$Ca_3Au_{14.26(6)}Ge_{4.74(5)}$	$Ca_3Au_{14.52(6)}Ge_{4.48(5)}$
e/a	1.93	1.87	1.86	1.78	1.75
f.w.	2991.59	3046.16	3201.26	3273.5	3304.93
space group, Z	$Im\bar{3}$, 8	$Im\bar{3}$, 8	$Im\bar{3}$, 8	$Im\bar{3}$, 8	$Im\bar{3}$, 8
latt. para. (Å)	14.670(1)	14.712(1)	14.764(5)	14.805(1)	14.8315(9)
vol.(Å^3)/d_{cal}(g/cm^3)	3157.4(4)/12.59	3184.3(4)/12.71	3217.9(17)/13.23	3244.8(5)/13.40	3262.5(3)/13.46
abs. coeff. (mm^{-1})	126.95	129.09	134.98	137.93	138.99
refl. coll./R_{int}	9936/0.0675	10106/0.0549	14192/0.1930	10707/0.0679	10116/0.0652
data/restr./para.	727/0/42	727/0/45	743/0/51	743/0/51	747/0/51
GOF on F^2	1.177	1.117	1.061	1.129	1.187
R1/wR2[$I > 2\sigma(I)$]	0.0229/0.0449	0.0355/0.0902	0.0575/0.0933	0.0354/0.0729	0.0398/0.0917
[all data]	0.0270/0.0458	0.0412/0.0931	0.0962/0.1023	0.0437/0.0758	0.0444/0.0941
res. peaks (e Å^{-3})[a]	2.124/−2.255	4.152/−3.351	5.322/−4.309	5.634/−4.256	5.785/−3.462

[a] The largest residual peaks are all around 0.7−1.4 Å from Au atoms.

analyses. Four parallel reactions with Yb replacing Ca were also carried out to resolve the uncertainty of assigning Ca or Ge to the special 2*a* site (below).

Table 1 summarizes the loaded proportions, reaction conditions, phase identities, and refined lattice parameters from both powder patterns and single crystals. All products are metallic in appearance, brittle, and evidently inert to moisture and air at room temperature.

X-ray Powder Diffraction. Phase analyses were made on the basis of powder diffraction data collected on a Huber 670 Guinier powder camera equipped with an area detector and Cu Kα_1 radiation (λ = 1.540598 Å). The detection limit of a minor phase with this instrument and system is conservatively estimated to be about 5 vol % in equivalent scattering power. Therefore, a seemingly pure product is denoted with at least a 95% yield. Phase identification was done with the aid of PowderCell,[29] and lattice parameter refinements were performed using UnitCell.[30] The lattice parameters refined from powder data were used with single crystal refinement results for bond distance calculations.

Single-Crystal X-ray Diffraction. Single crystals were mounted on a Bruker APEX CCD single crystal diffractometer equipped with graphite-monochromatized Mo Kα (λ = 0.71069 Å) radiation. Room temperature intensity data were collected in an ω scan method over 2θ = ∼3−57° range and with exposures of 10−30 s per frame. Data integration, Lorentz polarization, empirical absorption, and other corrections were made by SAINT and SADABS subprograms included in the SMART software package.[31] Full-matrix least-squares refinements on F_o^2 were performed with the aid of the SHELXTL v 6.1 program.[32]

Seven Ca- and two Yb-based crystals were structurally characterized in this work. However, results for only five Ca crystals (**1**−**5**) are reported in the text as representative, whereas structural data for two more Ca- (**s1** and **s2**) and the two Yb-containing phases (**s3** and **s4**) are given in the Supporting Information. All positional data were standardized by program STRUCTURE TIDY[33] and sorted to aid comparisons. The crystallographic, data collection, and structure refinement parameters for **1**− **5** are given in Table 2, and the refined positional and isotropic−equivalent displacement parameters are in Table 3. The remaining crystallographic data (cif) are available in the Supporting Information.

Direct methods were used to set up initial structural models, generally with eight independent sites. Two other weakly scattering Au/Ge8 and Au32 split sites (Table 3) were located on the basis of difference Fourier maps. The assignment of only a Ca atom to a Wyckoff 2*a* site in the center of the dodecahedra in crystals **1**, **2**, **3**, **s1**, and **s3** should be noted. The solution of structure **1** is described as an example. The Wyckoff 2*a* (0, 0, 0) site in **1** could be assigned to either Ca or Ge, with refined occupancies of 0.92 (4) or 0.53 (2), respectively. These yielded two slightly different compositions, $Ca_{3.23(1)}Au_{12.5}Ge_{5.5}$ or $Ca_3Au_{12.5}Ge_{5.633(5)}$, in which the overall atomic percentages varied by only ∼1.1% in Ca or 0.07% in Ge for the two extremes. According to experience, such small variations are about the same level as uncertainties for general EDS instruments. Therefore, no EDS data were collected with the aim to differentiate Ca or Ge for this purpose. Rather, the uncertainty was resolved by the structural solution for crystal **s3**, $Yb_{3.25}Au_{12.5}Ge_{5.39(3)}$, in which the atom on the 2*a* site could be unambiguously assigned to pure Yb. Therefore, Ca was also assigned to 2*a* site in crystals **2**, **3**, **s1**, and **s3**. From the viewpoint of surroundings, Ca fits in those dodecahedra better than Ge as far as the center-to-vertex distance, ∼ 3.6 Å. In addition, assignment of electropositive metal atoms to the 2*a* site was previously reported for $Yb_{25.05(3)}Zn_{146.83(9)}$ (= $Yb_{3.18}Zn_{18.35}$) and $Yb_{25.39(2)}Zn_{138.2(3)}Al_{7.7(3)}$ (= $Yb_{3.24}Zn_{17.28}Al_{0.96}$).[23]

Electronic Structure Calculations. The crystallographic data for crystal **1** were input directly as a model of the $Ca_{3.25}(Au,Ge)_{18}$ phase. However, the model of the $Ca_3(Au,Ge)_{19}$ phase required some modification because straightforward linear-muffin-tin-orbital (LMTO) calculations can only handle disorder-free structural models. Therefore, the structure of crystal **4** was simplified as follows: atoms in the sequence 1 to 4 were assumed being fully occupied by Au1 to Au4, and in the sequence 5−8 by Ge5−Ge8. Moreover, the minor split site (Au32) was omitted. As before,[16,18,19,34] subspace group *I*23 was used to circumvent the problem arising because of the disordered tetrahedron. All of these approximations resulted in a $Ca_3Au_{12.5}Ge_{6.5}$ model. The e/a (2.02) for this model is much larger than in the real crystal **4** though (1.78).

Calculations were performed by means of the self-consistent, tight-binding, LMTO method in the local density (LDA) and atomic sphere (ASA) approximations, within the framework of the DFT method.[35−38] The ASA radii of Ca, Au, and Ge were automatically scaled to 3.74, 3.00, and 2.75 Å (as average values) using the limitation of 18% maximum overlap between neighboring ASA spheres. One independent empty sphere was introduced to the

(29) Roisnel, T.; Rodríguez-Carvajal, J. WinPLOTR: a Windows tool for powder diffraction patterns analysis. In *Materials Science Forum, Proceedings of the Seventh European Powder Diffraction Conference* (*EPDIC 7*), Barcelona, Spain, May 20−23, 2000; Delhez, R., Mittenmeijer, E. J., Eds.; 2000; pp 118−123.
(30) Holland, T. J. B.; Redfer, S. A. T. *Miner. Mag.* **1997**, *61*, 65.
(31) *SMART*; Bruker AXS, Inc., Madison, WI, 1996.
(32) *SHELXTL*; Bruker AXS, Inc, Madison, WI., 2000.
(33) Gelato, L. M.; Parthé, E. *J. Appl. Crystallogr.* **1987**, *20*, 139.
(34) Ishii, Y.; Fujiwara, T. *Phys. Rev. Lett.* **2001**, *87*, 206408.
(35) Tank, R.; Jepsen, O.; Burkhardt, A.; Andersen, O. K. *TB-LMTO-ASA Program*, Vers. 4.7; Max-Planck-Institut für Festkörperforschung: Stuttgart, Germany, 1994.
(36) Shriver, H. L. *The LMTO Method*; Springer-Verlag: Berlin, Germany, 1984.
(37) Jepsen, O.; Snob, M. *Linearized Band Structure Methods in Electronic Band-Structure and its Applications, Springer Lecture Notes*; Springer Verlag: Berlin, Germany, 1987.
(38) Andersen, O. K.; Jepsen, O. *Phys. Rev. Lett.* **1984**, *53*, 2571.

Table 3. Atomic Coordinates and Isotropic Equivalent Displacement Parameters for $Ca_{3.25}(Au,Ge)_{18}$ (**1** and **2**), $Ca_{3.05(2)}Au_{13.67(8)}Ge_{5.33(6)}$ (**3**), and $Ca_3(Au,Ge)_{19}$ (**4** and **5**)

atom[a]	Wyck.	occ.	x	y	z	U_{eq}
			$Ca_{3.25}Au_{12.50}Ge_{5.50}$ (**1**)			
Au1	48 h	1	0.1037(1)	0.3368(1)	0.1965(1)	0.014(1)
Au2	24 g	1	0	0.4027(1)	0.3548(1)	0.010(1)
Au3	16f	1	0.1420(1)	x	x	0.013(1)
Au4	12d	1	0.4003(1)	0	0	0.016(1)
Ge5	24 g	1	0	0.2302(1)	0.0866(1)	0.011(1)
Ge6	12e	1	0.1989(1)	0	1/2	0.012(1)
Ge7	8c	1	1/4	1/4	1/4	0.019(1)
Ca8	2a	1	0	0	0	0.047(3)
Ca9	24 g	1	0	0.1888(2)	0.3060(2)	0.009(1)
			$Ca_{3.25}Au_{12.94(4)}Ge_{5.06(2)}$ (**2**)			
Au1	48 h	1	0.1040(1)	0.3376(1)	0.1980(1)	0.026(1)
Au2	24 g	1	0	0.4026(1)	0.3554(1)	0.020(1)
Au31	16f	0.956(3)	0.1427(1)	x	x	0.030(1)
Au32	16f	0.044(3)	0.188(1)	x	x	0.030(1)
Au4	12d	1	0.4013(1)	0	0	0.027(1)
Au/Ge5	24 g	0.145/0.855(8)	0	0.2317(2)	0.0844(1)	0.027(1)
Ge6	12e	1	0.1997(2)	0	1/2	0.018(1)
Ge7	8c	1	1/4	1/4	1/4	0.040(2)
Ca8	2a	1	0	0	0	0.082(10)
Ca9	24 g	1	0	0.1881(3)	0.3055(3)	0.019(1)
			$Ca_{3.05(2)}Au_{13.69(8)}Ge_{5.31(6)}$ (**3**)			
Au1	48 h	1	0.1043(1)	0.3389(1)	0.2005(1)	0.023(1)
Au2	24 g	1	0	0.4024(1)	0.3561(1)	0.017(1)
Au31	16f	0.968(5)	0.1468(1)	x	x	0.032(1)
Au32	16f	0.032(5)	0.1896(6)	x	x	0.032(1)
Au4	12d	1	4040(2)	0	0	0.025(1)
Au/Ge5	24 g	0.34/0.66(1)	0	0.2378(2)	0.0845(2)	0.026(1)
Ge6	12e	1	0.2001(4)	0	1/2	0.018(1)
Ge7	8c	1	1/4	1/4	1/4	0.046(3)
Au/Ge8a	24 g	0.05/0.28(1)	0	0.068(2)	0.071(2)	0.098(10)
Ca8b	2a	0.22(7)	0	0	0	0.017[b]
Ca9	24 g	1	0	0.1870(5)	0.3057(5)	0.017(2)
			$Ca_3Au_{14.26(6)}Ge_{4.74(5)}$ (**4**)			
Au1	48 h	1	0.1040(1)	0.3400(1)	0.2019(1)	0.014(1)
Au2	24 g	1	0	0.4023(1)	0.3570(1)	0.008(1)
Au31	16f	0.921(3)	0.1497(1)	x	x	0.030(1)
Au32	16f	0.079(3)	0.0956(7)	x	x	0.030(1)
Au4	12d	1	0.4047(1)	0	0	0.015(1)
Au/Ge5	24 g	0.435/0.565(8)	0	0.2374(1)	0.0834(1)	0.016(1)
Ge6	12e	1	0.2016(2)	0	1/2	0.010(1)
Ge7	8c	1	1/4	1/4	1/4	0.045(2)
Au/Ge8	24 g	0.153/0.181(9)	0	0.0799(6)	0.0680(6)	0.065(3)
Ca9	24 g	1	0	0.1857(3)	0.3047(3)	0.008(1)
			$Ca_3Au_{14.52(6)}Ge_{4.48(5)}$ (**5**)			
Au1	48 h	1	0.1038(1)	0.3406(1)	0.2021(1)	0.028(1)
Au2	24 g	1	0	0.4023(1)	0.3575(1)	0.022(1)
Au31	16f	0.905(4)	0.1524(1)	x	x	0.049(1)
Au32	16f	0.095(4)	0.0920(7)	x	x	0.049(1)
Au4	12d	1	0.4048(1)	0	0	0.028(1)
Au/Ge5	24 g	0.485/0.515(9)	0	0.2364(1)	0.0825(1)	0.031(1)
Ge6	12e	1	0.2020(2)	0	1/2	0.021(1)
Ge7	8c	1	1/4	1/4	1/4	0.072(2)
Au/Ge8	24 g	0.187/0.147(9)	0	0.0862(4)	0.0669(4)	0.054(2)
Ca9	24 g	1	0	0.1856(3)	0.3040(3)	0.022(1)

[a] For comparison, atoms in different structures are sorted in the same order and each independent atom is named in a sequence number for all sites rather than of that for each atom type. [b] Isotropic displacement parameter was fixed at the value for Ca9 because of its large correlation with occupancy.

$Ca_3(Au,Ge)_{19}$ model and none for $Ca_{3.25}(Au,Ge)_{18}$. Reciprocal space integrations were carried out by means of the tetrahedron method. Down-folding[39] techniques for outer Ca 4p, Au 5f, and Ge 4d orbitals were applied. Scalar relativistic corrections were automatically included in the calculations. The band structure was sampled for $24 \times 24 \times 24$ k points in the irreducible wedge of the Brillouin zone.

(39) Lambrecht, W. R. L.; Andersen, O. K. *Phys. Rev. B* **1986**, *34*, 2439.

Results and Discussion

Partial Ca−Au−Ge Phase Diagram. Currently six ternary phases have been reported in the Ca−Au−Ge

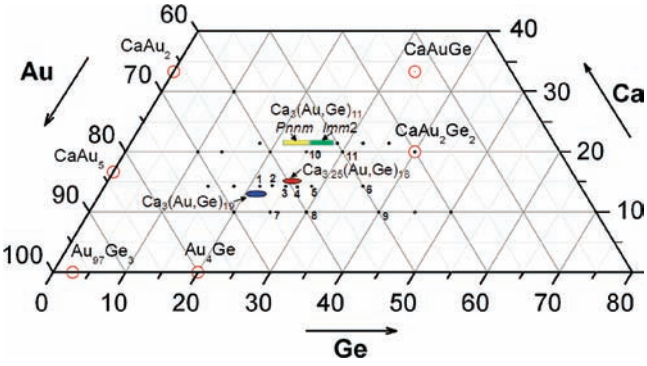

Figure 1. Partial Ca−Au−Ge phase diagram section at 400−500 °C showing relative phase regions. Blue and red ellipses mark the new phases **I** and **II**. Small black dots represent the samples investigated, as numbered in Table 1.

system, CaAuGe (*C*2/*m*), CaAuGe (*Pnma*), $CaAu_{1.24}Ge_{0.76}$ (*Imm*2),[40] $CaAu_2Ge_2$ (*I*4/*mmm*),[41] $Ca_3Au_{7.16-7.43}Ge_{3.84-3.57}$ (*Imm*2), and $Ca_3Au_{7.5-8.01}Ge_{3.5-2.99}$ (*Pnnm*).[27] The present YCd_6-type derivatives $Ca_3Au_{14.3-14.5}Ge_{4.7-4.5}$ ($Im\bar{3}$) and $Ca_{3.25}Au_{12.5-12.9}Ge_{5.5-5.1}$ ($Im\bar{3}$) are new members. In addition, we have also found $CaAu_3Ge$ (*Pa*3)[28] in this system (Table 1), which is isostructural with $CaAu_3Ga$.[24]

Although both $Ca_3Au_{14.3-14.5}Ge_{4.7-4.5}$ (**I**) and $Ca_{3.25}Au_{12.5-12.9}Ge_{5.5-5.1}$ (**II**) may have larger phase widths, the compositions refined from representative single crystals are probably very close to respective phase boundaries according to the comparative lattice parameters given in Table 1. Accordingly, the 500 °C section of the partial phase diagram is shown in Figure 1 with the respective phase fields and the compositions studied (Table 1) marked. As can be seen, the phase widths of **I** (red) and **II** (blue) are very small, and their composition differences are only about 5−10 at %. However, they are clearly separated from each other. More demonstrations of the phase separation are given below in terms of lattice and atomic parameters, valence electrons, and so forth.

Figure 2a shows the experimental powder pattern of the products from reaction 2, which lies between the subject, phases **I** and **II**. As seen, the experimental powder pattern is well fit by the patterns calculated from single crystal data sets **1** and **4** (with refined lattice constants of course), indicating the presence of a mixture of only **I** and **II**. Similar results are obtained according to the powder pattern of $Yb_{15.3}Au_{58.9}Ge_{25.9}$ (reaction 15), Figure 2b. Fittings of the entire mixed patterns from reactions 3 and 13 are also shown in Supporting Information, Figure S1. All of these results indicate that **I** and **II** are equilibrium phases in the temperature range used, 400−500 °C. In addition, it should be noted that the two structural types, distinctive in their innermost disordered tetrahedron versus an isolated M atom, can also be easily distinguished according to the intensity of the (110) reflections.[14] Supporting Information, Figure S2 shows this for the products of reactions 7 and 5, which are substantially pure **I** and **II**, respectively. The intensity of (110) peak ($2\theta \cong 8.4°$) is only ~1.4% of the strongest reflection ((543), 35.3°)

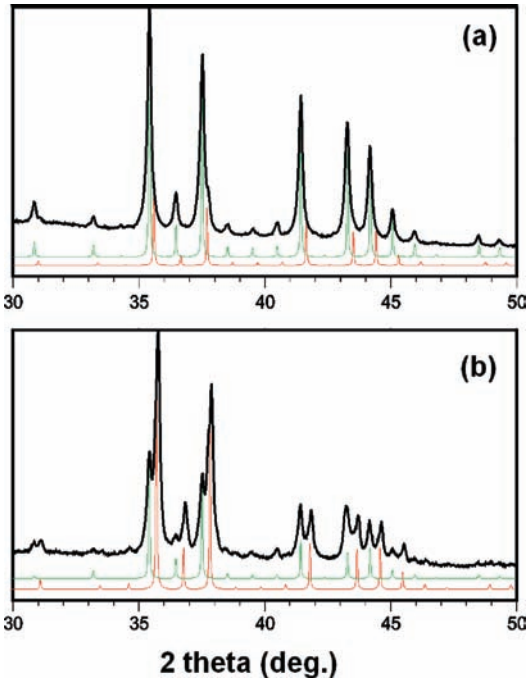

Figure 2. Experimental (black) powder patterns of (a) $Ca_{14.3}Au_{62.5}Ge_{23.1}$ and (b) $Yb_{15.3}Au_{58.9}Ge_{25.9}$. Red and green curves are simulated using single crystal data for **1** and **4**, and **s3** and **s4**, respectively, together with their respective lattice constants (Table 1).

if a tetrahedron exists in the dodecahedron; on the contrary, it is ~30% if a single atom is present.

To our knowledge, paired products of spinodal decomposition[42−44] also have the *same* symmetry and *similar* compositions, although a key factor for the occurrence of a spinodal decomposition is a negative second derivative of free energy with respect to composition.[45] With this in mind, samples that produce mixtures of $M_{3.25}(Au,Ge)_{18}$ and $M_3(Au,Ge)_{19}$ (M = Ca, Yb) deserve further microscopic examinations because they may be occur as spinodal pairs, at least from the viewpoint of structure, symmetry, and composition.

Crystal Structures. Actually, the shell geometries discussed below are common structural motifs for all YCd_6-type structures and their derivatives. Therefore, we will describe only the defect-free structure refined for crystal **1** (type **II**), which shows apparent complete chemical ordering between Au and Ge. Then the major structural differences among the other crystals studied will be pointed out.

Figure 3 shows the multiply endohedral clusters in $Ca_{3.25}Au_{12.5}Ge_{6.5}$ (**1**). The first shell, (a) a dodecahedron, is defined by 12 Ge5 and 8 Au3 atoms, with the latter on 3-fold axes. A single Ca atom lies at the cluster center, different from that in parent YCd_6. The average center-to-vertex distance for this shell is 3.61 Å, ~ 0.5 Å larger than other Ca−Au or Ca−Ge separations in the same structure. Thus Ca can be considered "rattling" in the dodecahedron, as also indicated by its larger displacement parameters (Table 3). Whether this "rattling" atom results in a good

(40) Merlo, F.; Pani, M.; Canepa, F.; Fornasini, M. L. *J. Alloys Compd.* **1998**, *264*, 82.
(41) May, N.; Schaefer, H. *Z. Naturforsch.* **1972**, *27b*, 864.
(42) Cahn, J. W. *J. Chem. Phys.* **1965**, *42*, 93.
(43) Ditchek, B.; Schwartz, L. H. *Annu. Rev. Mater. Sci.* **1979**, *9*, 219.
(44) Miyazaki, T. *Process., Prop. Appl. Met. Ceram. Mater., Proc. Int. Conf.* **1992**, *1*, 13.
(45) Gibbs, J. W. *Scientific Papers of J. Willard Gibbs*; New York: Dover, 1961; Vol. *2*, p 105, 252.

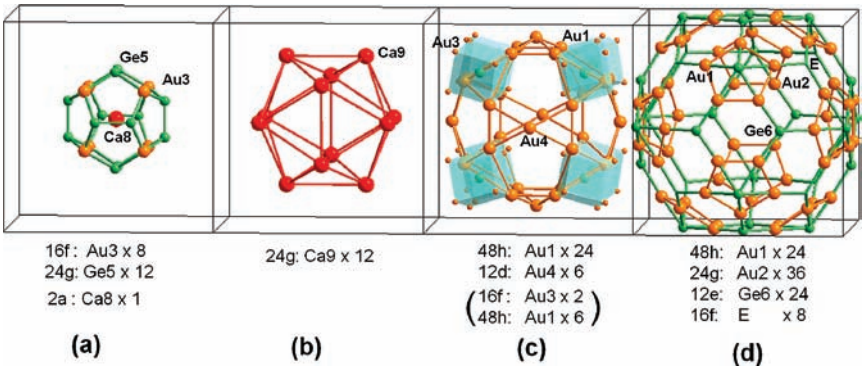

Figure 3. Multiply endohedral polyhedral clusters in defect-free $Ca_{3.25}Au_{12.5}Ge_{5.5}$ (Z = 2). (a) Ca8-centered Au_8Ge_{12} dodecahedron, (b) Ca_{12} icosahedron, (c) Au_{30} icosidodecahedron, plus eight Au_8 cubes (cyan, each consisting of 2 Au3 + 6 Au1) centered by Ge7 (green), (d) $Ge_{24}E_8$ triacontahedron (E = empty vertex). Each of 60 triacontahedral edges is centered by an Au atom.

thermoelectric candidate as do Skutterudites[46] or not is beyond this work. All pentagonal faces of the Au_8Ge_{12} dodecahedron are outwardly capped by Ca9 atoms, which define a larger Ca_{12} icosahedron (b) as the second shell. This is the only shell in the structure completely defined by electropositive atoms. The center-to-vertex distance of this shell is 5.27 Å, and the surface Ca9−Ca9 separations are about 5.55 Å, meaning that they have no significant bonding to each other. Rather, they have strong interactions with the neighboring Au and Ge on pentagonal faces of both the inner dodecahedral and the next 30-atom icosidodecahedral shell (c). The last is defined by only Au atoms (24 Au1 + 6 Au4), all in a sphere with average radii ~5.90 Å. The direct interactions among these Au atoms are not strong, as indicated by the intracluster distances $d_{Au1-Au1}$ = 3.04 Å and $d_{Au1-Au4}$ = 3.39 Å. However, they have pronounced bonding interactions with Ge5 on the dodecahedral shell and Au1, Au2, and Ge6 atoms on the outmost triacontahedral shell (d), as indicated by the shorter intercluster separations, Au1−Ge5, 2.71 Å; Au4−Ge5, 2.80 Å; Au1−Au2, 2.87 Å; Au1−Au3, 3.02 Å; Au2−Au4, 2.95 Å; and Au4−Au4, 2.93 Å. The outermost triacontahedral shell consists of 32 vertices and 60 edges, with center-to-vertex distances in the range of 7.77−7.86 Å. The decoration of the triacontahedral shell is noteworthy: of the 32 ideal vertices, the eight with real 3-fold symmetry are empty, and the others are unexceptionally occupied by Ge6 atoms. On the other hand, 60 Au atoms locate on all midedges of the triacontahedron.

The interstitial Ge7 atoms always present at the Wyckoff 8*c* site (0.25, 0.25, 0.25) are alien to the parent YCd_6.[9] These are sandwiched between the icosidodecahedral and the triacontahedral shells, with strong bonding interactions with Au1 which is a member of both ($d_{Au1-Ge7}$ = 2.62 Å). Actually, each Ge7 also strongly interacts with Au3 atoms on the 3-fold axis of the dodecahedral shell, as indicated by the bond distance $d_{Au3-Ge7}$ = 2.74 Å. Thus each Ge7 is enclosed in an Au_8 cube, as shown Figure 3c.

The above structural motifs basically apply for all crystals studied in this work (**2**−**5**, **s1**−**s4**), except that (1) disordered tetrahedra of Au/Ge8 atoms occur within the dodecahedral shells in crystals **3**−**5**, **s2**, and **s4** (as in the parent YCd_6), each atom at one-third occupancy; (2)

(46) He, T.; Chen, J.; Rosenfeld, D. H.; Subramanian, M. A. *Chem. Mater*. **2006**, *18*, 759.

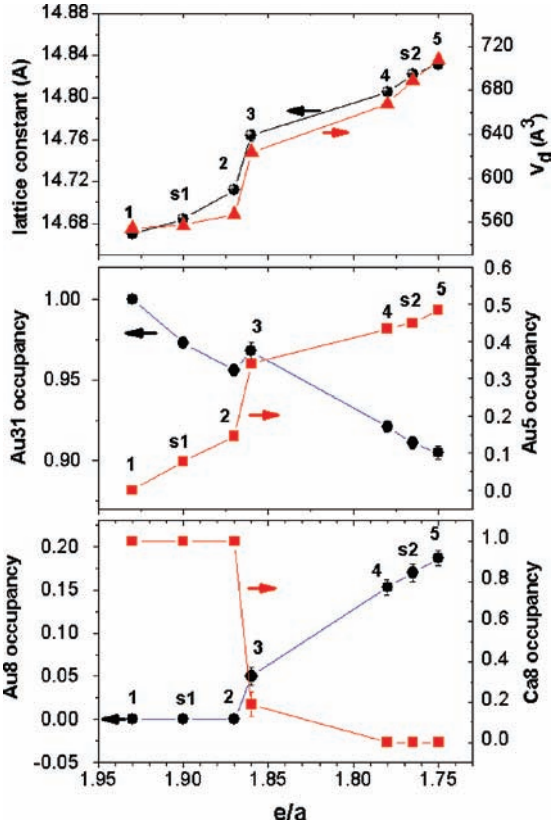

Figure 4. Plots of (a) lattice parameters and calculated volumes of dodecahedra, (b) refined Au occupancies at Au31 and Au/Ge5 sites, and (c) Au occupancies at Au/Ge8 site or Ca occupancies at Ca8 site as a function of valence electron counts per atom (e/a). The group of larger e/a values (left) pertain to type **II** crystals, $Ca_{3.25}(Au,Ge)_{18}$, the smaller e/a (right), to type **I**, $Ca_3(Au,Ge)_{19}$.

the 16*f* sites in all other crystals but **1** are split into two unequal components; (3) the sites equivalent to Ge5 (24*g*) in **1** are occupied by Au/Ge mixtures with increasing Au proportions; (4) both 48*h* and the site equivalent to Ge5 (24*g*) in **1** split into two parts in crystal **s4**, a special case.

In summary, crystals **1**, **2**, **s1**, and **s3** have same general formula of $M_{3.25}(Au,Ge)_{18}$ (**II**), whereas crystals **4**, **5**, **s2**, and **s4**, of $M_3(Au,Ge)_{19}$ (**I**), each with some small nonstoichiometry. Obviously, they are two different derivatives of YCd_6. As for $Ca_{3.05(2)}Au_{13.69(8)}Ge_{5.31(6)}$ (**3**), the fact that it refined with both the customary disordered

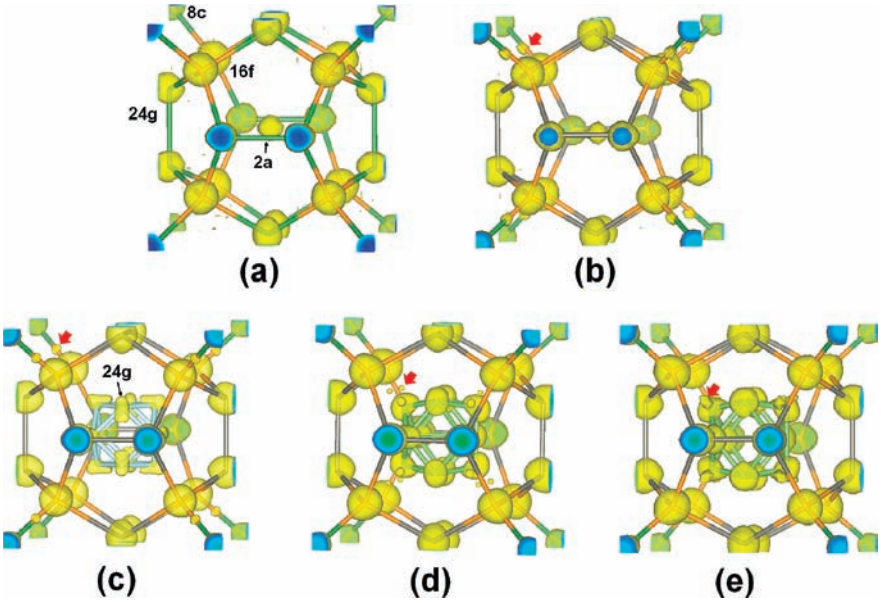

Figure 5. 3-D Fourier maps of electron densities around the origin in crystals: (a) **1**, (b) **2**, (c) **3**, (d) **4**, and (e), **5**, respectively. Representative Wyckoff positions are labeled, and the minor split densities around 16*f* sites are marked with red arrows. The cutoff contour level is 14.0 e/Å^3. (The blue shadings represent core densities in the forward facing sections.).

tetrahedron and a fractional Ca (~ 22(7)%) within the dodecahedron likely means it is a weakly modulated or intergrown crystal of both $Ca_{3.25}(Au,Ge)_{18}$ and $Ca_3(Au,Ge)_{19}$. The data set's large intensity averaging factor (R_{int} = 0.193) probably relates to this effect (Table 2). However, co-refinement of both a tetrahedron and a single atom within dodecahedron is not new; rather, it was first reported for $YbZn_{5.86}$ and $Yb(Zn,Al)_{5.75}$.[23] Nevertheless, we believe that crystal **3** is an intermediate state between $Ca_{3.25}(Au,Ge)_{18}$ and $Ca_3(Au,Ge)_{19}$, as supported by the following.

Systematic Structural Changes. The seven Ca-based crystal structures (**1**−**5**, **s1**, and **s2**) provide useful clues regarding the evolution of different structural parameters as a function of the overall valence electron count per atom (*e*/*a*, assuming 1 *e* for Au). As shown in Figure 4a, the lattice parameters generally increase as *e*/*a* decreases, consistent with the increase in Au and decrease in Ge proportions in corresponding formulas (Table 2). As we know, Ge is smaller and electron richer and Au is larger in size and electron poorer. However, small cusps or inflections appear in all of the data over an *e*/*a* range of 1.86 and 1.79, in contrast to the smooth changes before (**1** → **s1** → **2**) and afterward (**4** → **s2** → **5**). These indicate that a phase or other transition may occur between **2** and **4**. Actually, single crystal X-ray results support this conclusion because crystals **1**, **s1**, and **2** belong to the $Ca_{3.25}(Au,Ge)_{18}$ structure **II** stoichiometrically whereas **4**, **s2**, and **5**, to the $Ca_3(Au,Ge)_{19}$ structure **I**. The occurrence of a presumably first-order phase transition is also supported by the volume changes for the dodecahedron (Figure 4a), the discontinuous Au occupancies at Au31 and Au/Ge5 (Figure 4b) sites, and the Au (or Ca) occupancies at Au/Ge8 (or Ca8) sites (Figure 4c), which exhibit either upward or downward inflections at the same *e*/*a* region, ~1.86 or below.

Figure 4 also reveals that the formation of crystals in the $Ca_{3.25}(Au,Ge)_{18}$ versus the $Ca_3(Au,Ge)_{19}$ family show strong correlations between lattice parameters and *e*/*a* values. The $Ca_{3.25}(Au,Ge)_{18}$ phase exists only in a region with $e/a \geq 1.86$ and $a < \sim 14.72$ Å under our synthetic conditions, whereas $Ca_3(Au,Ge)_{19}$ forms in a region with $e/a \leq 1.79$ and $a > \sim 14.80$ Å (Figure 4a). In addition, these plots give clues about disorder and atomic decorations in both families. For example, the Au occupancy at the Au31 site (the major split part) tends to decrease from **1** to **5** (Figure 4b), in contrast, opposite changes are found for Au at Au/Ge5 and Au/Ge8 sites (Figures 4b and 4c). We will discuss the split phenomenon in more detail in the following section.

Disorder within the Dodecahedra. From Table 3 and Supporting Information, Table S2, we know that the following types of disorder are observed among the present phases: an atom splitting at the 16*f* Au3 site, an occupancy disorder/mixing at Au/Ge5 and Au/Ge8 sites, and an orientational disorder at the Au/Ge8 site. All of these occur within the dodecahedral shell. Figure 5a−5e show the observed electron densities about and within this shell for crystals **1**−**5**, respectively.

As shown, the 16f Au3 sites split into two unequal parts for crystals **2**−**5**. Close examination reveals an interesting image: for **2** and **3**, small fractions (3−4%) refined outside of the dodecahedron (Figures 5b and 5c). On the contrary, small densities (8−10%) lie within the dodecahedron in **4** and **5** (Figures 5d and 5e). The relative positions of the split sites, the sizes of the dodecahedra, and their contents are correlated: small dodecahedral volumes, < 570 Å^3 (Figure 4a), accompany its occupation by a single (Ca) atom, and the minor part of 16*f* is located outside the dodecahedron. On the other hand, a Au/Ge tetrahedron together with the minor split portion are enclosed within dodecahedra with volumes > 660 Å^3.

Electronic Structures. Figure 6 shows the densities-of-states (DOS) of (a) $Ca_{3.25}Au_{12.5}Ge_{5.5}$ (**II**, $e/a = 1.93$) and (b) $Ca_3Au_{12.5}Ge_{6.5}$ (the model for **I**, $e/a = 2.02$). Basically, both patterns are quite similar although some core-like states between −10 eV and −8 eV split in (b). In both patterns, Au 5d populations lie within a range of −8 to −3 eV,

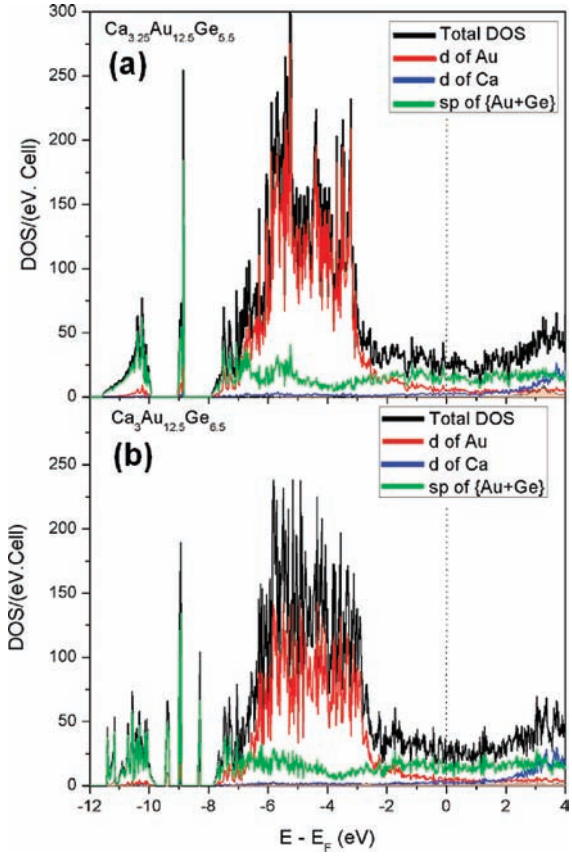

Figure 6. Calculated densities-of-states (DOS) of (a) $Ca_{3.25}Au_{12.5}Ge_{5.5}$ (**II**) and (b) a $Ca_3Au_{12.5}Ge_{6.5}$ model (**I**). The projected DOSs for Ca8 and Ge_4 tetrahedra in the dodecahedra are shaded in orange at the bottom of the plots, respectively.

whereas s and p states of Au and Ge dominate below this. The Au/Ge s and p states also spread across the Fermi energy (E_F). In contrast, the Ca 3d orbitals lie mainly above E_F. The small contributions of Ca and of the Ge_4 tetrahedron within the dodecahedral shell are represented by orange-shaded areas at the bottom of (a) and (b), respectively. The Ca states populate a high energy region (2−4 eV), with minor contributions at or below E_F, whereas the Ge_4 states spread thinly over a large energy range.

In contrast to the DOS curves for "$Ca_3Au_{11.5}In_{6.5}$"[18] and "$Ca_3Au_{11}Ga_8$",[19] which are bona fide ACs and exhibit pseudogaps at about E_F, there is no apparent pseudogap for either of the present phases. This may explain our failure to find any Ca−Au−Ge quasicrystal.

Remarks

Exploration of new YCd_6-type quasicrystals and approximants continues to yield surprising results beyond imagination. This study also establishes that stable YCd_6-type structures and derivatives continue to the east in the Periodic Table. Members of this family in different proportions span from binary Zn and Cd phases[47] (with two valence electrons) to ternary triels[18,19] (three electrons), and now to the tetrels (four electrons). How valence electrons and size are reconciled and how structures are regularized in this family are not a trivial matter.

We have previously noticed that (a) stuffed YCd_6-type structures can have 3:19 stoichiometries as well, for example, $Ca_3(Au,Ga)_{19}$,[19] and (b) a large mismatch in atom sizes in these may result in the disappearance of the tetrahedron, as in $YbZn_{5.8}$.[23] However, the coexistence of both effects in our systems is a surprise. The discoveries of $M_3(Au,Ge)_{19}$ (**I**) and $M_{3.25}(Au,Ge)_{18}$ (**II**) (M = Ca, Yb) provide an unprecedented playground in which studies of important factors that govern phase formation and stability become possible, as discussed. These also raise the opportunity to probe some related and inspired "unknowns", for example, the effect of "rattling" Ca within the dodecahedral shell versus thermoelectric properties, the possible occurrences of spinodal decompositions, and of modulation or intergrowth as well. The fact that both $Ca_3(Au,Ge)_{19}$ and $Ca_{3.25}(Au,Ge)_{18}$ exhibit the YCd_6-type structural motif rather than $Mg_{32}(Al,Zn)_{49}$ type, as does $Na_{13}Au_{20}Ge_{7.5}$[26] as well, is also striking.

Finally, the discoveries of $Ca_3(Au,Ge)_{19}$ and $Ca_{3.25}(Au,Ge)_{18}$ open a new and exciting challenge: Does any QC exist in the presence of a corresponding AC that is isostructural with $Ca_{3.25}(Au,Ge)_{18}$, or even with nothing in the cluster center?

Acknowledgment. This research was supported by the U.S. National Science Foundation, Solid State Chemistry, via Grants DMR-0444657 and −0853732. All of the work was performed in the facilities of the Ames Laboratory, U.S. Department of Energy.

Supporting Information Available: Tables S1−S2, Figures S1−S2, and detailed CIF data. This material is available free of charge via the Internet at http://pubs.acs.org.

(47) Villars, P.; Calvert, L. D. *Pearson's Handbook of Crystallographic Data for Intermetallic Phases*, 2nd ed.; American Society of Metals: Materials Park, OH, 1991; Vol. *1*.